Corneal Edema in Inducible Slc4a11 Knockout Is Initiated by Mitochondrial Superoxide Induced Src Kinase Activation

Diego G Ogando , Edward T Kim , Shimin Li , Joseph A. Bonanno *

Posted Date: 15 May 2023

doi: 10.20944/preprints202305.1059.v1

Keywords: corneal enendothelial dystrophy; Slc4a11; barrier function; lactate transporters; Src kinase; oxidative stress; Visomitin

Article

Corneal Edema in Inducible Slc4a11 Knockout Is Initiated by Mitochondrial Superoxide Induced Src Kinase Activation

Diego G. Ogando, Edward T. Kim, Shimin Li and Joseph A. Bonanno *

Vision Science Program, School of Optometry, Indiana University, Bloomington, IN;
digogand@indiana.edu (D.G.O.); edtkim@indiana.edu (E.T.K.); shimli@indiana.edu (S.L.)
* Correspondence: Correspondence: jbonanno@indiana.edu

Abstract: Purpose: Inducible Slc4a11 KO leads to corneal edema by disruption of the pump and barrier functions of the corneal endothelium (CE). The loss of Slc4a11 NH_3-activated mitochondrial uncoupling leads to mitochondrial membrane potential hyperpolarization-induced oxidative stress. The goal of this study is to investigate the link between oxidative stress and failure of pump and barrier functions and test different approaches to revert the process. **Methods**: Mice homozygous for Slc4a11 Flox and Estrogen receptor –Cre Recombinase fusion protein alleles at 8 weeks of age were fed Tamoxifen (Tm) enriched chow (0.4 g/Kg) for 2 weeks, and controls were fed normal chow. During the initial 14 days, Slc4a11 expression, corneal thickness (CT), stromal [lactate], Na^+-K^+ ATPase activity, mitochondrial superoxide levels, expression of lactate transporters, and activity of key kinases were assessed. In addition, barrier function was assessed by fluorescein permeability, ZO-1 tight junction integrity, and cortical cytoskeleton F-actin morphology. **Results**: Tm induced a rapid decay in Slc4a11 expression that was 84% complete at 7 days and 96% at 14 days of treatment. Superoxide levels increased significantly by day 7; CT and fluorescein permeability by day 14. Tight junction ZO-1 distribution and cortical cytoskeleton were disrupted at day 14 concomitant with decreased expression of Cldn1 yet an increase in tyrosine phosphorylation. Stromal lactate increased by 60%, Na^+-K^+ATPase activity decreased by 40%, and expression of lactate transporters MCT2 and MCT4 significantly decreased, but MCT1 was unchanged at 14 days. Src kinase was activated but not Rock, PKCα, JNK, or P38Mapk. Mitochondrial antioxidant Visomitin (SkQ1, mitochondrial targeted antioxidant) or Src kinase inhibitor eCF506 significantly slowed the increase in CT, with concomitant decreased stromal lactate retention, improved barrier function, reduced Src activation and Cldn1 phosphorylation, and rescued MCT2 and MCT4 expression. **Conclusions**: Slc4a11 KO-induced CE oxidative stress triggered increased Src kinase activity that results in perturbation of pump components and barrier function of the CE.

Keywords: corneal endothelial dystrophy; Slc4a11; barrier function; lactate transporters; Src kinase; oxidative stress; Visomitin

1. Introduction

Homozygous and compound heterozygous mutations in Solute Linked Cotransporter A11 (SLC4A11) cause Congenital Hereditary Endothelial Dystrophy (CHED)[1], marked by corneal edema and eventual endothelial cell death in early childhood. SLC4A11 is an NH_3-sensitive electrogenic H^+ transporter localized to the basolateral membrane and the inner mitochondrial membrane of corneal endothelial cells [2, 3]. Basolateral plasma membrane SLC4A11 is postulated to contribute to the corneal endothelial pump function by an H^+ buffering mechanism that enhances lactate transport [4]. More significantly, inner mitochondrial membrane SLC4A11 is an NH_3-sensitive mitochondrial uncoupler that protects corneal endothelial cells by suppressing mitochondrial superoxide production during glutamine catabolism by preventing hyperpolarization of the mitochondrial membrane potential [3]. In Slc4a11-deficient mouse corneal endothelial cells, inhibiting superoxide production by reducing ammonia production, treating with a mitochondrial uncoupler, or direct mitochondrial antioxidant treatment, prevented cell death in the presence of

 doi:10.20944/preprints202305.1059.v1

glutamine, indicating that mitochondrial superoxide production was the primary factor in inducing cell death[3, 5].

In the conventional Slc4a11 KO mice, corneal edema is observed early (<12 weeks of age) with mild changes in cell morphology, yet no significant difference in corneal endothelial cell density compared to wild type [6, 7]. However, at later ages, cell morphology becomes more aberrant and cell density significantly decreases in the KO [6, 7]. In Slc4a11 KO mice, the gene is null during embryonic development, and edema is present at eye-opening, which precludes uncovering the sequence of early events leading to edema. To circumvent this problem, we have generated an inducible Slc4a11 KO mouse model that recapitulates the conventional KO phenotype over time[8]. In addition to mitochondrial superoxide production, there are losses in Na^+-K^+ ATPase activity and expression of key lactate transporters (monocarboxylate cotransporter MCTs) in this KO. The goal of the current study was to investigate the earliest events within corneal endothelial cells that ultimately lead to edema. Our working hypothesis is that mitochondrial oxidative stress is the initial trigger that leads to alterations in gene expression, cell morphology, permeability, corneal edema, and eventual cell death.

In the inducible Slc4a11 KO model, we found that mitochondrial oxidative stress precedes corneal edema, lactate accumulation (pump function failure), and a disruption of the barrier function. The loss of the pump function was associated with a decrease in Na^+-K^+ ATPase activity and decreased expression of lactate transporters. The failure of barrier function is associated with an altered cortical cytoskeleton, mis-localization of ZO1, reduced Cldn1 expression, and increased levels of phosphorylated Src kinase. Topical eye-drop treatment with mitochondrial-targeted antioxidant (Visomitin; SkQ1) or Src-kinase inhibitor (eCF506) rescued the phenotype, indicating that oxidative stress and downstream Src-kinase activation results in perturbation of pump and barrier function in this model.

2. Materials and Methods

Drugs

All drugs: Visomitin, #HY-100474, eCF506, #HY-112096, and Ripasudil, #HY-15685 were obtained from MedChemExpress.

Mice and Therapies

Generation of the inducible Slc4a11 KO mouse was described previously[8]. Slc4a11 Flox/Flox mice were obtained from Ozgene. Cre-ERT2 mice (Stock No: 008463) were obtained from Jackson Laboratories. In this strain, ubiquitous Cre-ERT2 expression is directed by a strong promoter. $Slc4a11^{Flox/Flox}$ //CreERT2/CreERT2 mice at 8 weeks of age were fed with Tamoxifen (Tm) enriched chow (0.4g/kg, Envigo #TD130859) for two weeks, followed by normal chow. Whole body Slc4a11 KO is expected in this model. Genotyping procedures for Slc4a11 flox and for CreERT2 alleles were described previously[8]. The non-specific effects of Tamoxifen on corneal thickness were insignificant [8]. Central corneal thickness was measured by Optical Coherence Tomography as described in detail previously[8]. Eye drop therapy was performed as follows: Visomitin (SkQ1) 1.5 µm in PBS, eCF506 1 µM in PBS or PBS, 10 µl drops were applied thrice/day (9 am, 1 pm, 5 pm) in both eyes to $Slc4a11^{Flox/Flox}$ //CreERT2/CreERT2 mice at 8 weeks of age starting at the same time of Tamoxifen feeding. In addition, central corneal thickness was measured before and at 14 days of treatment. Mice were euthanized by inhalation of carbon dioxide followed by cervical dislocation at different time points and corneas obtained for analysis. All mice were housed in pathogen-free conditions and used in the experiments in accordance with Indiana University institutional guidelines (BIACUC Approval #21-013) and the current regulations of the National Institutes of Health, the United States Department of Agriculture and the Association for Research in Vision and Ophthalmology (ARVO) Statement for the Use of Animals in Ophthalmic and Vision Research.

 doi:10.20944/preprints202305.1059.v1

QPCR

QPCR was performed as described previously[8]. Briefly, corneal endothelium-Descemet's membrane (CEDM) was dissected from whole corneas using jeweler's forceps from three mice and were pooled to obtain one sample. Three Ctrl and three Tm samples were subjected to QPCR. Slc4a11 primers: Forward: CTGTGAGGTTCGCTTTGT, Reverse: GTGCCAGTCTTCAGGAGC. Beta actin primers: CTAAGGCCAACCGTGAAA, Reverse: ACCAGAGGCATACAGGGA.

Stromal Lactate

Corneas were obtained, and epithelium and endothelium were removed. Individual stromas were placed in pre-weighed Eppendorf tubes, pulverized in liquid nitrogen, and homogenized in 30 µl of PBS using a plastic disposable pestle. The sample was centrifuged at 15,000 g for 15 minutes at 4°C. The supernatant was recovered. The remaining pellet was dried at 60°C within a vacuum centrifuge for two hours and weighed (dry weight). Lactate was measured in the supernatant using a fluorescent kit (Abcam #ab65330) according to the manufacturer's instructions.

Endothelial Permeability Assay

Whole corneas were dissected and placed on plates within small dimples endothelial side up. A volume of 10 µl of 0.1% sodium fluorescein in bicarbonate-rich Ringer (BR) was added on the endothelial side and incubated at room temperature for 30 minutes. The corneas were washed thrice for five minutes each with 10 µl BR. After removing all liquid, corneas were positioned in wells of a 96-well plate, and fluorescence (excitation: 485 nm, emission: 520 nm) was measured in a microplate reader. As a positive control, corneas were incubated for one hour with 10 µl EGTA 2 mM in Ca-free PBS before incubation in fluorescein.

Na^+-K^+ ATPase Activity

Two corneal endothelial-Descemet membrane (CEDM) peelings from the same mouse were pooled and homogenized in 30 µl assay buffer provided by ATPase Assay kit (Abcam #ab234055) using plastic disposable pestle. After sonication the sample was centrifugated at 10,000 g for 10 minutes at 4°C. The supernatant was recovered, and phosphates in the sample were depleted by incubation in 40 µl of PiBind resin (Innova Biosciences #501-0015) for 15 minutes at room temperature in a rotary device. After centrifugation at 1,000 g for two minutes the sample was recovered, and ATPase activity was measured in 5 µl of sample in the presence or absence of 1 mM ouabain. Na^+-K^+ ATPase activity was obtained by subtracting the activity in presence of ouabain from the total activity. Protein was measured by BCA method.

Mitochondrial Superoxide

Following euthanasia, corneas were dissecte, maintained in Hanks Balanced Salt Solution at 37°C, and stained with MitoSOX (Thermo Fisher Scientific #M36008) 1 µM in HBSS for 30 minutes at 37°C and washed 3 times for 5 minutes in HBSS. To facilitate identifying the endothelial cells, nuclei were stained with Hoechst 1 µg/ml for 10 minutes at room temperature and then washed 3 times for 5 minutes in HBSS. Corneas were flattened by performing 4 relaxing cuts and positioned with the endothelial surface facing down in a glass bottom Petri Dish (MetTek #P35G-1.5-20-C) in 100 ul of HBSS. An 18 mm coverslip was placed over the cornea with a plastic weight to flatten the tissue. Images were taken with a Zeiss Observer Z1 microscope using a 40X objective. Five images were taken for each cornea. Using Image J, the mean fluorescence intensity of each individual cell was obtained and then averaged per image and cornea.

 doi:10.20944/preprints202305.1059.v1

Immunofluorescence

Immunofluorescence was performed as previously described[8]. Primary antibody: Mouse anti-ZO-1 (1:100) (Thermo Fisher Scientific #33-9100). Phalloidin-A488 (Thermo Fisher Scientific #A12379) 1X solution was used to stain F-actin.

Immunoprecipitation

Immunoprecipitation was performed following instructions from the Pierce Classic Immunoprecipitation kit (Thermo Fisher Scientific #26146). Briefly, two CEDM from one mouse were pooled and lysed in 30 µl of IP Lysis buffer supplied by the kit supplemented with protease plus phosphatase inhibitors. Five µl of lysate were saved to use as input. In a spin column provided by the kit, 25 µl of lysate was combined to 475 µl of IP Lysis buffer and pre-clear with 20 µl of Control Agarose slurry for one hour at 4°C in a rotary device. The immune complex was prepared by combining the 500 µl of pre-cleared diluted lysate with 1 µg of rabbit P-tyrosine antibody (Cell Signaling Technology #8954S) or 1 ug of control rabbit IgG (Cell Signaling Technology #3900S) or 1 ug of control mouse IgG (Cell Signaling Technology #5415S) and incubating 18 hours at 4°C in a rotary device. The immune complex was captured by incubating the antibody/lysate sample with 20 µl of Protein A/G Agarose slurry for one hour at 4°C in a rotary device. The agarose containing the immune complex was washed four times with 200 µl of IP Lysis buffer and once with 1X Conditioning Buffer supplied by the kit. The complex is eluted by adding 10 µl of 2X Mastermix from the Protein Simple Jess kit and then boiling for 10 minutes. After centrifugation from 1,000 g for 1 minute, the eluted protein was recovered and used to run the western immunoassay for Cldn1 and ZO-1, as described below.

Western Immunoassay

Two CEDM peelings of one mouse were pooled and lysed in 25 µl RIPA lysis buffer containing protease plus phosphatase inhibitors. Protein was measured by BCA method. Equal amount of protein (1.5 µg) was loaded into wells of the 12 to 230 kDa separation module of a Protein Simple Jess system (Protein Simple, San Jose, CA, USA). Antibodies were added in the following dilutions: MCT1 (Abcam #ab90582) 1:10, MCT2 (Santa Cruz Biotechnologies #sc-166925) 1:10, MCT4 (Santa Cruz #sc-376465) 1:10, Atp1a1 (Abcam #ab760020) 1:10, Atp1b2 (Abcam #ab185210) 1:10, ZO-1 (Thermo Fisher Scientific #33-9100) 1:10, Cldn1 (Thermo Fisher Scientific #37-4900) 1:10, β-catenin (Cell Signaling Technology #9582) 1:10, P(S19)-MLC (Cell Signaling Technology #3671) 1:10, P-PKCα (Cell Signaling Technology #9375) 1:10, P-JNK (Cell Signaling Technology #9255S) 1:10, P-P38Mapk (Cell Signaling Technology #9215S) 1:10, Src (Cell Signaling Technology #2109) 1:50, P-Src (Cell Signaling Technology #6943) 1:10. Secondary antibodies and substrate were provided by the Jess kit. For normalization, total protein on each lane was quantified with Total Protein Module (Protein Simple #DM-TP01). Jess data are obtained as virtual blots in which molecular weight and signal intensity are presented. Results in the form of traditional electropherogram are also obtained with this approach.

Statistical Analysis

All corneal thickness measurements have at least 5 replicates. All other assays have at least 3 replicates. Results are presented as Mean ± SEM. Statistical analysis was done with GraphPad 9.4 (GraphPad Software, Inc.). For two groups comparison Student's t-test was performed. For three or more groups, One-way or Two-way ANOVA was performed followed by Tukey's multiple comparison test. Significance was defined as $p<0.05$.

3. Results

To study early events leading to corneal edema, Slc4a11 Flox/Flox // CreERT2/CreERT2 mice at 8 weeks of age were fed with tamoxifen (Tm) chow to induce Slc4a11 knock-out and different parameters were studied at several time points. Tm induced 84% and 96% Slc4a11 messenger RNA knock down in the endothelium at 7 and 14 days of Tm treatment, respectively (Figure 1A). Corneal

Preprints (www.preprints.org) | NOT PEER-REVIEWED | Posted: 15 May 2023 doi:10.20944/preprints202305.1059.v1

thickness was slightly higher at 7 days, but increased significantly by 14 days post Tm induction (Figure 1B). Since the underlying mechanism of the endothelial pump is lactate-linked water flux [9], we examined corneal [lactate] and lactate transporter (MCT1, 2, and 4) expression. Lactate accumulation in the stroma indicates inhibition of the corneal endothelial pump function. We found that lactate increased significantly at 7 days and remained higher than Control at 14 and 28 days of Tm induction (Figure 1C). Consistent with pump failure, there was a 40% reduction in Na^+-K^+ ATPase activity at 14 days post-Tm treatment (Figure 1D). At this same time point, we examined the expression of Na^+-K^+ATPase components and MCTs. Whereas there was no significant change in the expression of subunits Atp1a1 and Atp1b2 (Figure 2A-B) and no changes in MCT1 (Figure 2C), significant decreases in MCT2 and 4 were observed (Figure 2D-E).

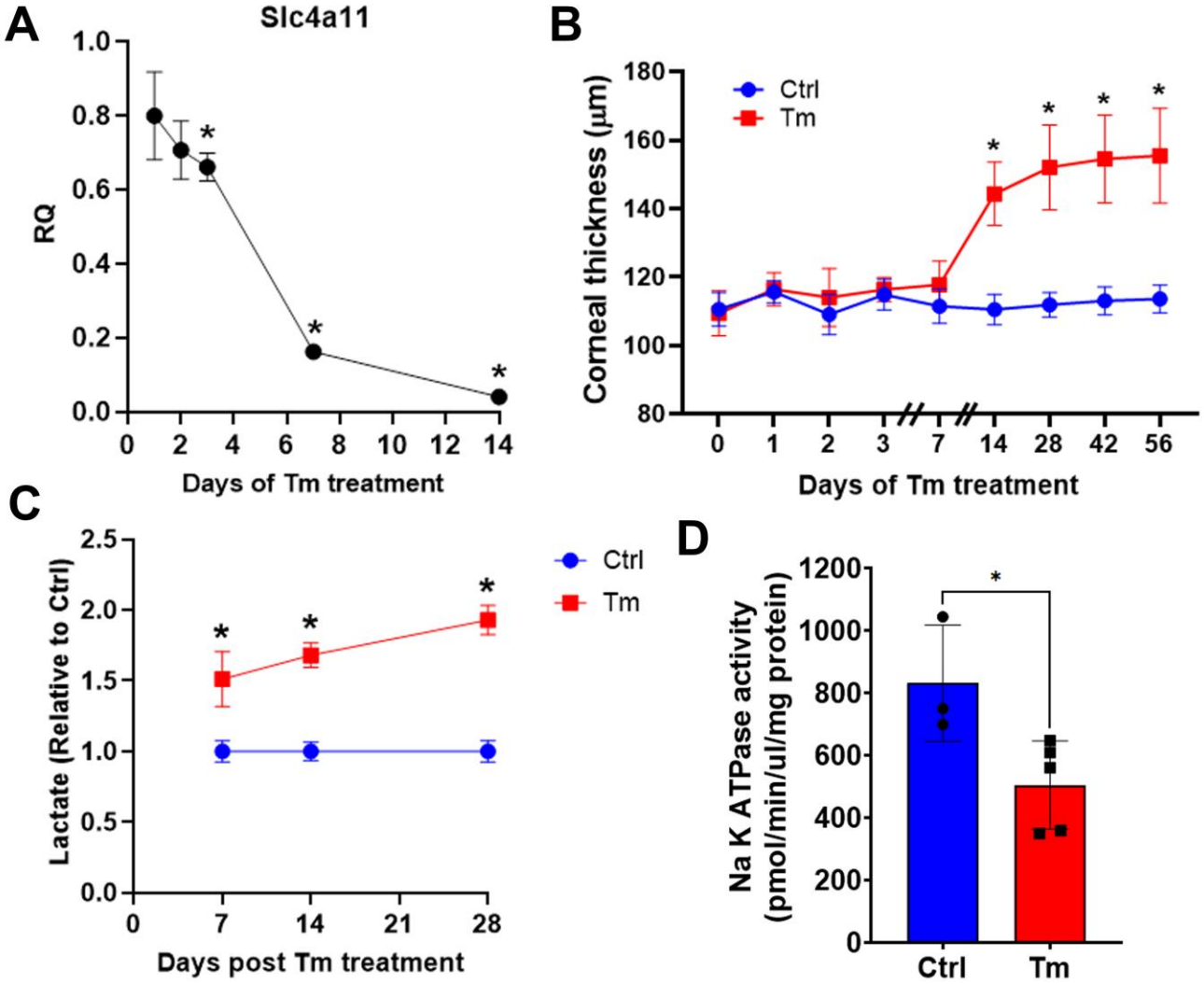

Figure 1. Changes in the pump function in the inducible Slc4a11 KO. **A**. Time course of relative Slc4a11 expression by QPCR in CEDM. Relative quantity ±SEM, n=3, *: P<0.05. **B**. Corneal thickness time course after Tm treatment; mean ± SEM, n=5, P<0.0001. **C**. Stomal lactate content; Relative values versus Control; mean ± SEM, n=3, *: P<0.05. **D.** Na^+-K^+ ATPase activity at 14 days of Tm treatment; mean ± SEM, n=3 (Ctrl) and n=5 (Tm), *: P<0.05.

Preprints (www.preprints.org) | NOT PEER-REVIEWED | Posted: 15 May 2023 doi:10.20944/preprints202305.1059.v1

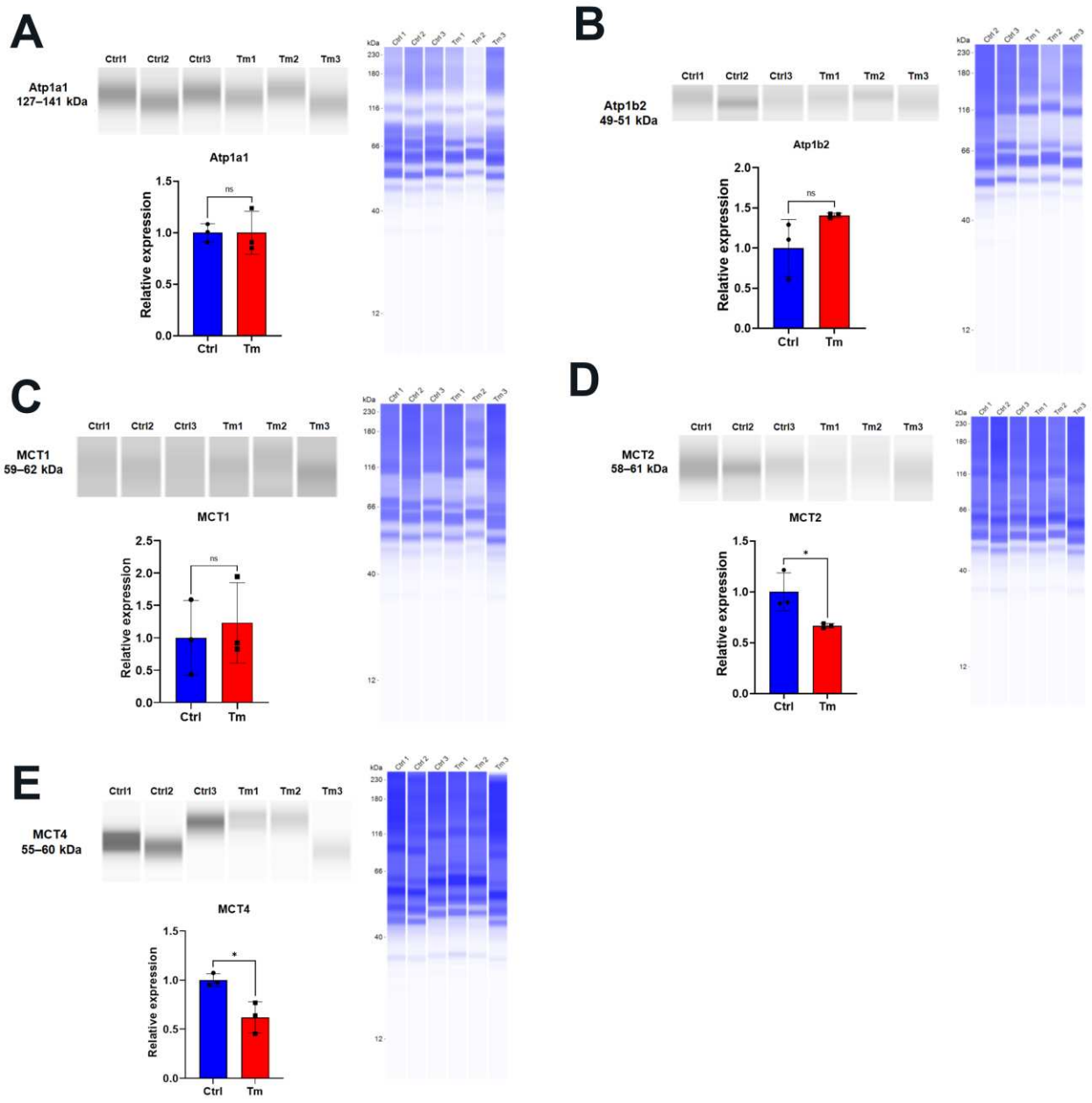

Figure 2. Lactate transporter expression is decreased in the inducible KO at 14 days of Tm treatment. Jess immunoassays: **A.** Atp1a1. **B.** ATP1b2. **C.** MCT1. **D.**MCT2. **E.** MCT4. Blue blot shows total protein. Relative values versus Control; mean ± SEM, n=3. *: P<0.05. ns=not significant.

Whereas the pump function consists of vectorial (stroma to anterior chamber) transport of lactate and water, maintenance of transendothelial osmotic gradients derived from the ion transport activity requires an intact osmotic barrier that is conferred by tight and adherens junctions. Therefore, we examined endothelial permeability and the protein expression associated with barrier function. The integrity of tight junctions (studied by ZO-1 staining) and cortical cytoskeletal (studied by F-actin) were altered at 14 days but was not noticeable at 7 days (Figure 3A). Similarly, endothelial permeability increased at 14 days, not at 7 days (Figure 3B). To explore potential changes in tight junction assembly that may explain the increase in permeability we examined expression of several junction proteins. Consistent with increased permeability at 14 days, Cldn1 levels were decreased, whereas ZO-1 levels were increased in Tm-treated mice, while β-catenin levels were not changed (Figure 3C).

Preprints (www.preprints.org) | NOT PEER-REVIEWED | Posted: 15 May 2023 doi:10.20944/preprints202305.1059.v1

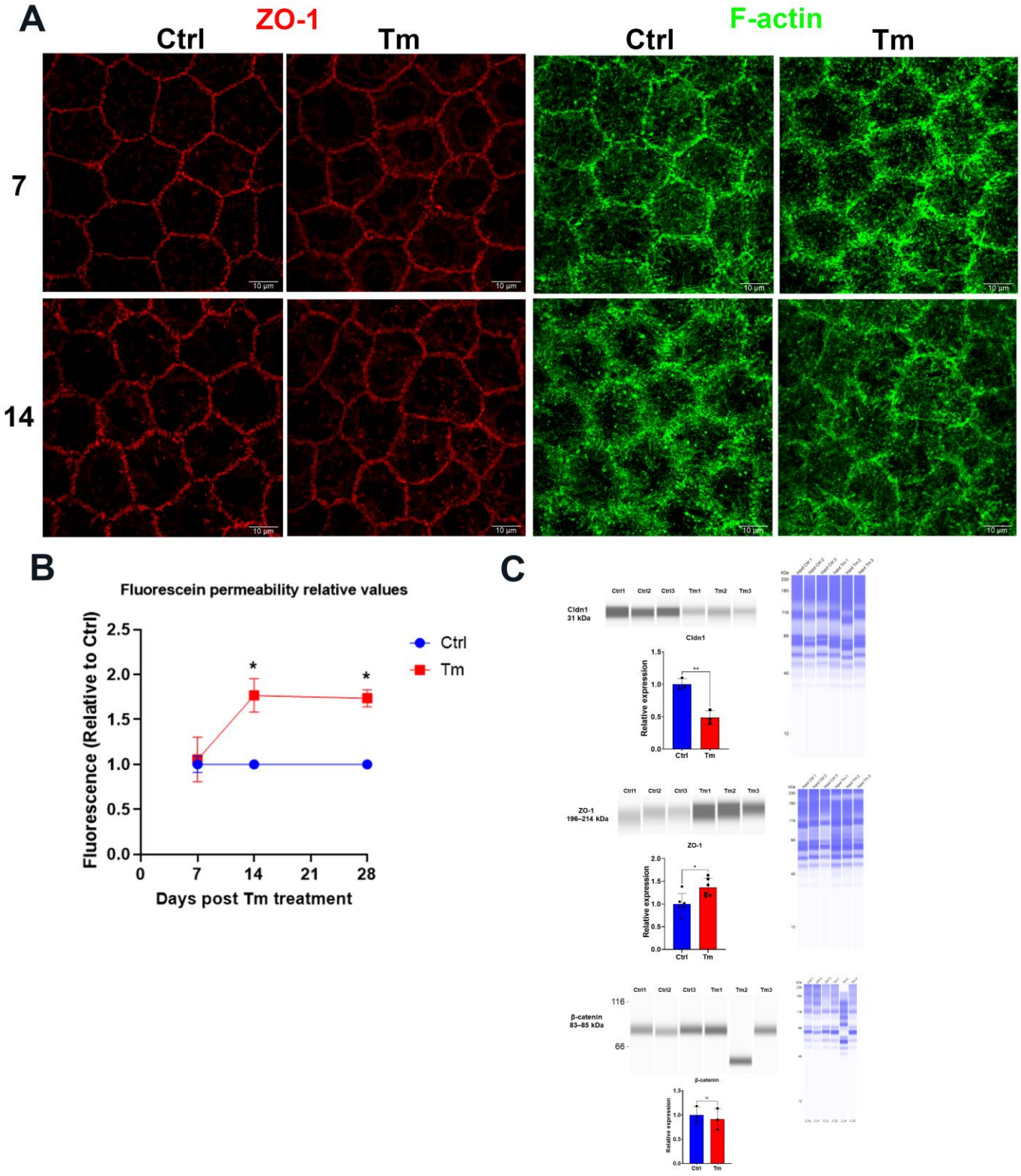

Figure 3. Tight junction and cortical cytoskeleton structure and endothelial permeability are altered at 14 days of Tm treatment. **A**. Representative images of ZO-1 and F-actin at 7 and 14 days of Tm treatment. **B**. Endothelial fluorescein permeability. Relative values versus control; mean ± SEM, n=3, *: P<0.01. **C**. Jess immunoassay of ZO-1, Cldn1 and β-catenin. Relative values versus Control; mean ± SEM, n=6 (ZO-1) and n=3 (Cldn1 and β-catenin). *: P<0.05. **: P<0.01. ns=not significant.

We hypothesized that a trigger for these changes in protein expression and subsequent corneal edema is the oxidative stress caused Slc4a11 deletion [3, 10]. We observed that mitochondrial

Preprints (www.preprints.org) | NOT PEER-REVIEWED | Posted: 15 May 2023 doi:10.20944/preprints202305.1059.v1

superoxide levels increase in the Tm group at 7 days when significant Slc4a11 knockdown occurs. Mitochondrial superoxide levels remained elevated at 14 days (Figure 4A & B). Thus, mitoROS production precedes the development of corneal edema.

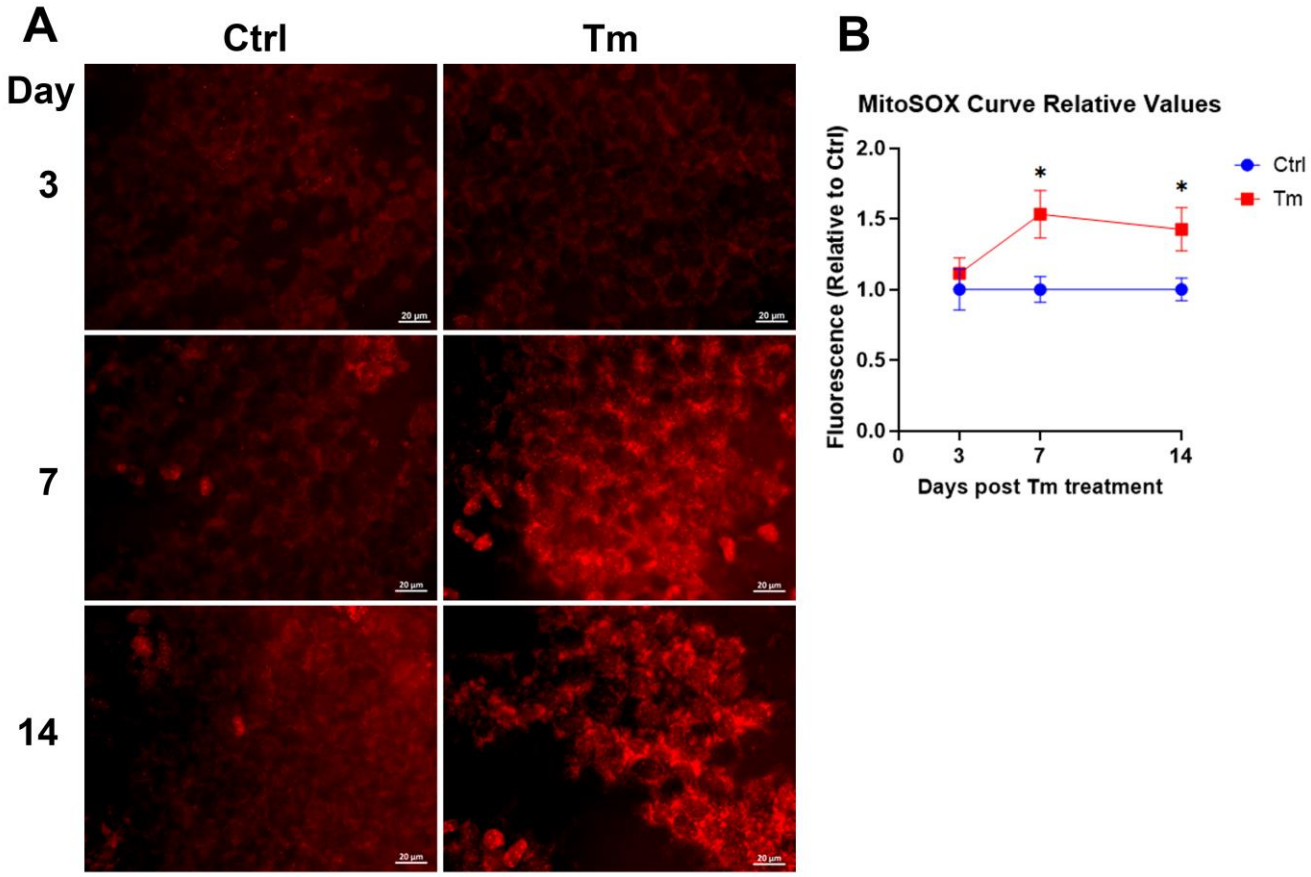

Figure 4. MitoROS coincides with Slc4a11 knock down and precedes corneal edema. **A**. Representative MitoSOX staining at 3, 7 and 14 days of Tm treatment. **B**. Quantification of MitoSOX staining. Relative values versus control; mean ± SEM, n=4, *: P<0.05.

Several kinases have been associated with ROS-induced disruption of the barrier function: Rock, MLCK, PKCα, JNK, c-SRC, and p38 MAP kinase [11-16]. ROCK or MLCK (tested by phosphorylation of MLC), PKCα, JNK and p38 MAP kinase were not activated by Tm at 14 days (Figure 5A-D). Only c-Src was activated at 14 days (Figure 5E). Src is implicated in tyrosine phosphorylation of ZO-1, Cldns, Ocldn, E-cadherin, N-cadherin, β-catenin, and other proteins of tight and adherens junctions [11, 17, 18]. Src kinase tyrosine phosphorylation can produce degradation or mislocalization of the junction components [11, 17]. Whereas ZO-1 tyrosine phosphorylation is decreased in Tm samples, (Figure 5F). Cldn1 tyrosine phosphorylation is increased, suggesting that Src kinase is mediating this event along with a decrease in Cldn1 protein level (Figures 5G and 3C).

Preprints (www.preprints.org) | NOT PEER-REVIEWED | Posted: 15 May 2023 doi:10.20944/preprints202305.1059.v1

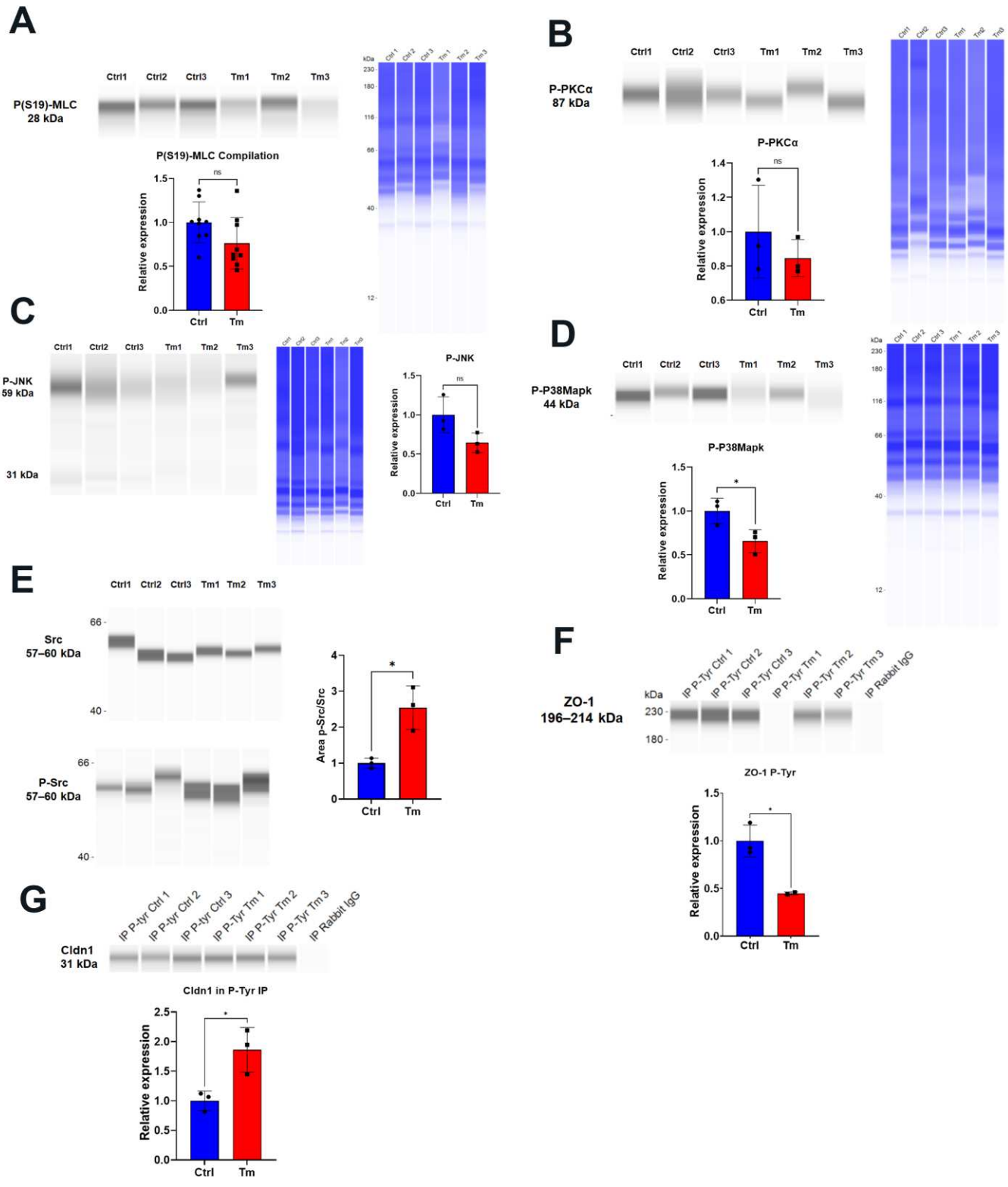

Figure 5. Src kinase is activated and Cldn1 tyrosine phosphorylation increases at 14 days post-Tm treatment. Jess immunofluorescence and quantification of: **A**. P(S19)-MLC, n=9. **B**. P-PKC*α*, n=3. **C**. P-JNK, n=3. **D**. P-P38Mapk, n=3, P<0.05. **E**. Src and P-Src, n=3, P<0.05. **F**. ZO-1 blot from P-tyrosine IP samples, for relative expression calculation, intensity values are normalized to input values found in Figure 2C middle panel and then to control values, n=3, P<0.05. **G**. Cldn1 blot from P-tyrosine IP samples, for relative expression calculation, intensity values are normalized to input values found in Figure 2C upper panel and then to control values, n=3, P<0.05.

 doi:10.20944/preprints202305.1059.v1

ROCK inhibitor topical therapy has been used to treat Fuchs Endothelial Corneal Dystrophy (FECD)[17]. Rho kinase activation can directly or indirectly result in MLC phosphorylation leading to actomyosin contraction and disruption of the barrier function[19]. We did not find increased MLC phosphorylation in our model. However, ROCK activation can be detrimental to the barrier and the pump function by mechanisms independent of increasing MLC phosphorylation [20]. For example, *ex vivo* treatment of corneal endothelium with Rho Kinase inhibitor Ripasudil increased the expression of proteins of the pump and barrier function [20]. For these reasons, we tested topical treatment with Ripasudil in our model. Topical administration of the drug (eye drops, thrice per day) had no effect on corneal thickness, fluorescein permeability, tight junctions, or cortical cytoskeleton (Figure 6 A-C).

Preprints (www.preprints.org) | NOT PEER-REVIEWED | Posted: 15 May 2023 doi:10.20944/preprints202305.1059.v1

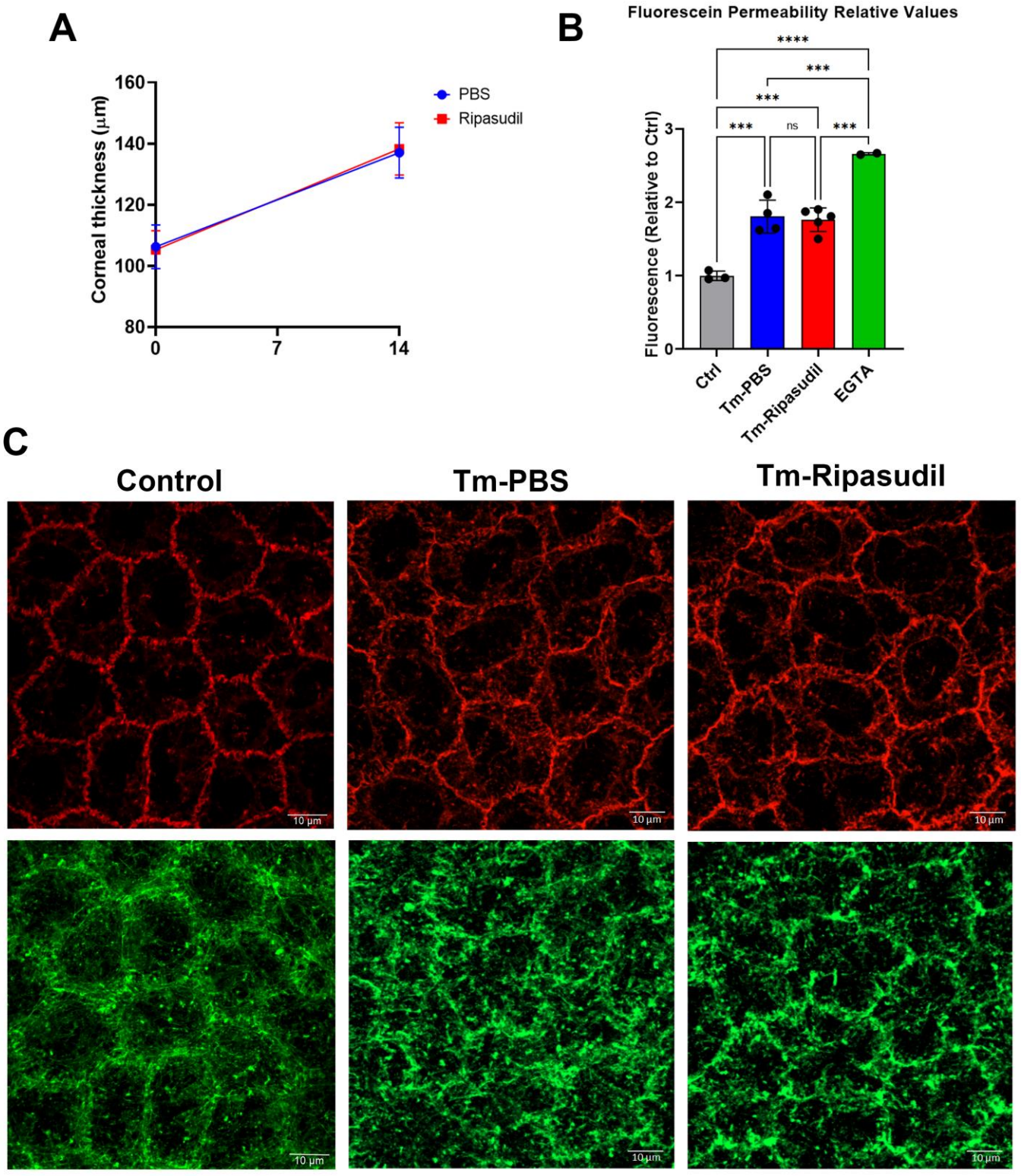

Figure 6. Ripasudil eye drop therapy had no effect on Slc4a11 KO-induced corneal edema. All measurements were performed at 14 days post-Tm treatment. **A**. Corneal thickness before and after Ripasudil or PBS eye drop therapy, n=5 for Ripasudil and n=4 for Control. **B**. Relative endothelial fluorescein permeability upon eye drop therapy measured at 14 days of Tm treatment, n=4 for Tm-PBS, n=5 for Tm-Ripasudil, n=3 for Control (not treated with Tm) and n=2 for EGTA. ***: P<0.001. **C**. Representative images of ZO-1 and F-actin at 14 days of Ripasudil or PBS eye drop therapy and Tm treatment.

 doi:10.20944/preprints202305.1059.v1

With evidence for induction of mitochondrial oxidative stress and c-Src kinase activation, we used Visomitin to reduce oxidative stress and eCF506 (Src Kinase inhibitor) to inhibit c-Src kinase activity directly in the mouse model via topical delivery. In both cases, eye drop therapy significantly reduced the increase in corneal thickness induced by Slc4a11 knockout, indicating that mitochondrial ROS and Src kinase mediated edema (Figure 7A). In addition, both drugs significantly inhibited the increase in permeability (Figure 7B) and lactate accumulation (Figure 7C) induced by Slc4a11 knockout. Moreover, topical Visomitin and eCF506 rescued tight junction (ZO-1) and opposed cortical cytoskeleton (F-actin) disorganization induced by Slc4a11 knockout (Figure 7D). Furthermore, Visomitin and eCF506 significantly decreased Src phosphorylation in the KO relative to control PBS drops (Figure 8A), indicating that mitochondrial oxidative stress triggers Src kinase activation. Both drugs reversed the decrease in Cldn1 levels and decreased Cldn1 tyrosine phosphorylation (Figure 8B-C). The drugs also recovered Slc4a11-induced decline in MCT2 (Figure 8D) and MCT4 (Figure 8E), and had no effect on MCT1 levels (Figure 8F).

Preprints (www.preprints.org) | NOT PEER-REVIEWED | Posted: 15 May 2023 doi:10.20944/preprints202305.1059.v1

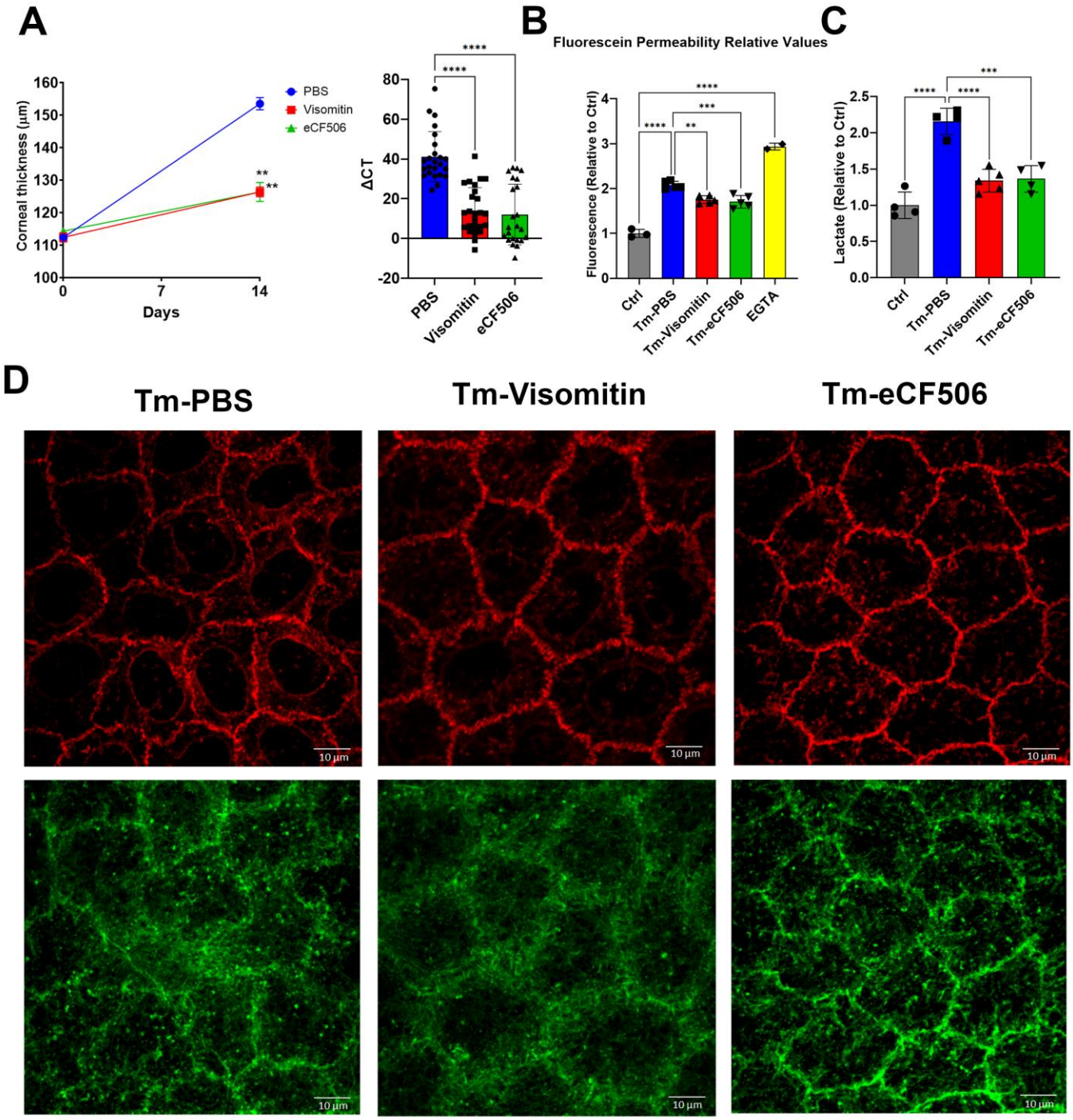

Figure 7. Visomitin and eCF506 eye drop therapies inhibit Slc4a11 KO-induced corneal edema. **A**. Corneal thickness and ΔCT after Visomitin, eCF506 or PBS eye drop therapy, n=12 (24 eyes) for PBS, n=13 (26 eyes) for Visomitin and n=12 (24 eyes) for eCF506. **: P<0.001, ***: P<0.0001. **B**. Relative endothelial fluorescein permeability upon eye drop therapy measured at 14 days of Tm treatment, n=5 for Tm-PBS, Tm-Visomitin and Tm-eCF506, n=3 for Control (not treated with Tm) and n=2 for EGTA. .**: P<0.01, ***: P<0.0001. **C**. Stomal lactate content at 14 days of Tm; Relative values versus Control; mean ± SEM, n=4 for Control, Tm-PBS and Tm-eCF506; and n=5 for Tm-Visomitin. ***: P<0.001, ****: P<0.0001. **D**. Representative images of ZO-1 and F-actin at 14 days of Visomitin, eCF506 or PBS eye drop therapy and Tm treatment.

Preprints (www.preprints.org) | NOT PEER-REVIEWED | Posted: 15 May 2023 doi:10.20944/preprints202305.1059.v1

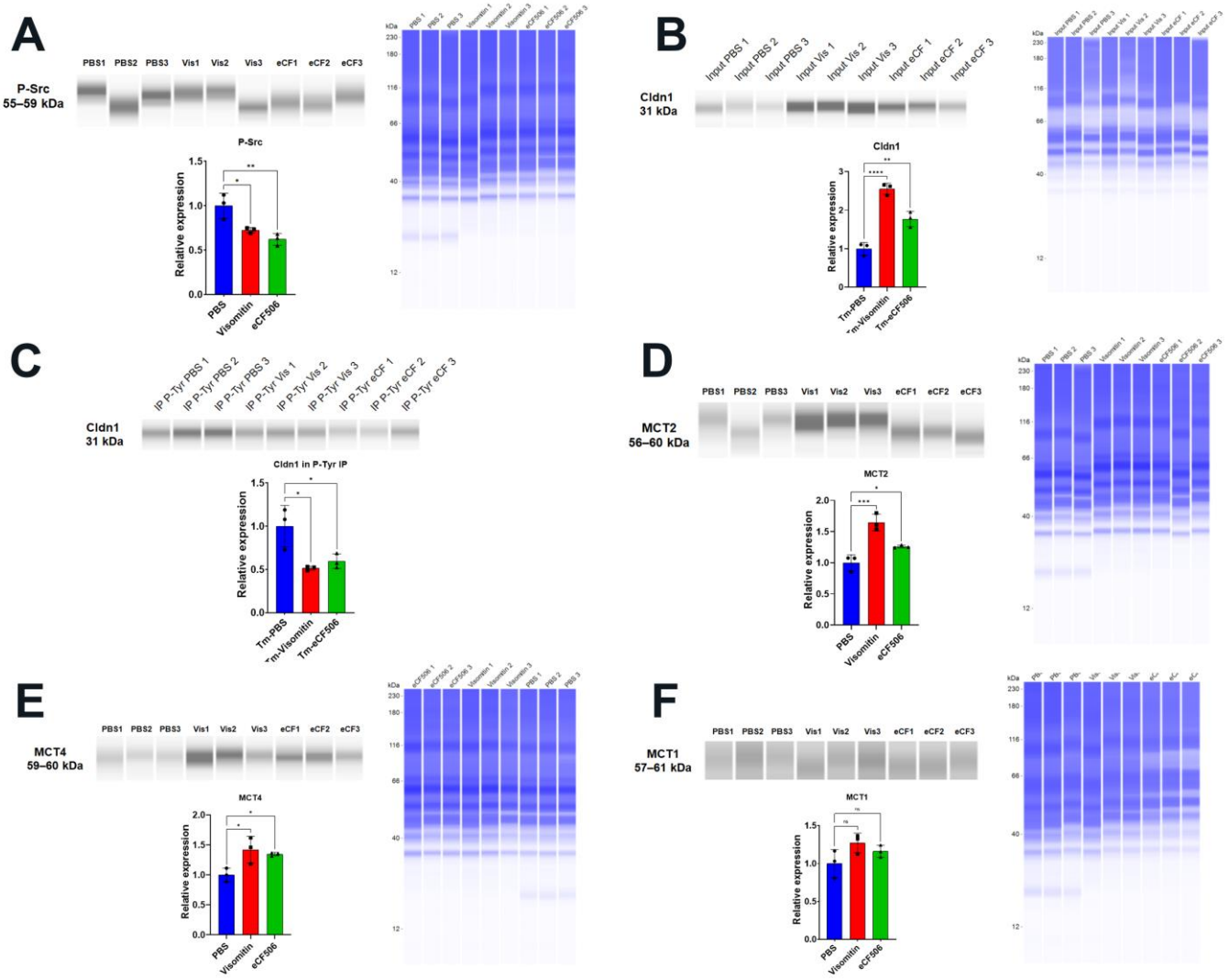

Figure 8. Visomitin and eCF506 eye drop therapy inhibits Src kinase and rescues expression of Cldn1, MCT2 and MCT4 at 14 days of Tm. Jess immunoassay and quantification. **A**. P-Src, n=3. *: P<0.05, **: P<0.01. **B**. Cldn1, n=3, **: P<0.01, ****: P<0.0001. **C**. Cldn1 blot from P-tyrosine IP samples, for relative expression calculation, intensity values are normalized to input values found in B and then to control values, n=3, *: P<0.05. **D**. MCT2, n=3, *: P<0.05, ***: P<0.001. **E**. MCT4, n=3, *: P<0.05. **F**. MCT1, n=3.

4. Discussion

In the current study, we find that mitochondrial oxidative stress precedes the development of edema in the inducible Slc4a11 KO. Pump function is altered by decreased levels of MCT2 and MCT4 and reduced Na^+-K^+ ATPase activity, leading to lactate accumulation in the stroma. Furthermore, barrier function is altered as indicated by elevated fluorescein permeability, breakdown of tight junction and cortical cytoskeleton, reduction in Claudin 1 levels and increased Cldn1 tyrosine phosphorylation via activation of c-Src kinase. MitoROS (i.e., superoxide) and Src Kinase appear to be the main players in the onset of edema as it was inhibited by Visomitin or eCF506.

In the Slc4a11 KO, the lack of NH_3-activated mitochondrial uncoupling hyperpolarizes the mitochondrial membrane potential leading to excessive superoxide production [3]. In the inducible KO, Visomitin eye drop therapy successfully reverted the edema, indicating that MitoROS is the primary cause of the phenotype. This is consistent with previous data showing a reduction in corneal edema in the conventional KO using MitoQ (a mitochondrial targeted antioxidant) i.p.[5] and Dimethyl αketoglutarate (bypass glutaminolysis which reduces MitoROS) topical therapy [3].

 doi:10.20944/preprints202305.1059.v1

Visomitin has been shown to improve dry eye symptoms [21, 22] and may be a good candidate for topical treatment in CHED or FECD.

Src kinase was activated in the KO. The changes in barrier function, increased fluorescein permeability, disorganization of tight junction and cortical cytoskeleton, tyrosine phosphorylation, and decreased levels of Claudin 1 were all reverted by Src kinase inhibitor topical therapy. Src kinase is known to be activated upon oxidative stress and impair the barrier function by tyrosine phosphorylation of tight and adherens junction proteins, resulting in their degradation or mislocalization in colon and bile duct epithelial cells [11, 17, 18]. Hydrogen peroxide directly activates Src by Tyrosine sulfenylation, that leads to Tyrosine 416 phosphorylation and activation[23].

ZO-1 localization was altered as observed by immunofluorescence. However, ZO-1 levels increased as tested by Western blot. This increase may be a compensatory response to tight junction disruption. ZO-1 tyrosine phosphorylation in Slc4a11 KO is decreased, indicating that Src kinase is unlikely to drive mislocalization of this protein.

We did not expect protection of the pump function (MCT2, MTC4 expression, and lactate levels) by Src inhibition. Src can increase TCA cycle and OXPHOS resulting in increased mitochondrial ROS production [24]. Therefore, Src inhibition could have decreased ROS production in our model. This could explain the protective effect of the Src inhibitor (eCF506). Alternatively, Src kinase could have activated an unknown kinase or transcription factor leading to the changes in the pump function. However, these hypotheses were not tested in the present study.

Consistent with the lack of activation of ROCK, topical Ripasudil treatment had no protective effect on corneal edema. Contrary to our observation, Rock and p38 MAP kinase are associated with disruption of the barrier function upon oxidative stress *in vitro* [25]. Ripasudil has been found to protect endothelium and promote wound healing after treatment of FECD patients with Descemet stripping only and in patients after cataract surgery [26, 27]. ROCK inhibitor Y-27632 increased the efficiency of cell-based therapy of FECD[28]. In our study we found no activation of PKCα, JNK, or p38 MAP kinases.

Figure 9 summarizes the sequence of events leading up to formation of corneal edema. Slc4a11 deficiency increases the proton motive force producing excess MitoROS. ROS directly activates Src kinase, which phosphorylates tight and adherens junction proteins leading to their degradation or mislocalization. Cortical cytoskeleton alterations are induced as a secondary response and the end result is a perturbation of the barrier function. The specific mechanism of impairment of MCT cotransporter expression and Na^+-K^+ATPase activity, a feature of this model[8, 29], via oxidative stress is unknown and will require further study.

Preprints (www.preprints.org) | NOT PEER-REVIEWED | Posted: 15 May 2023 doi:10.20944/preprints202305.1059.v1

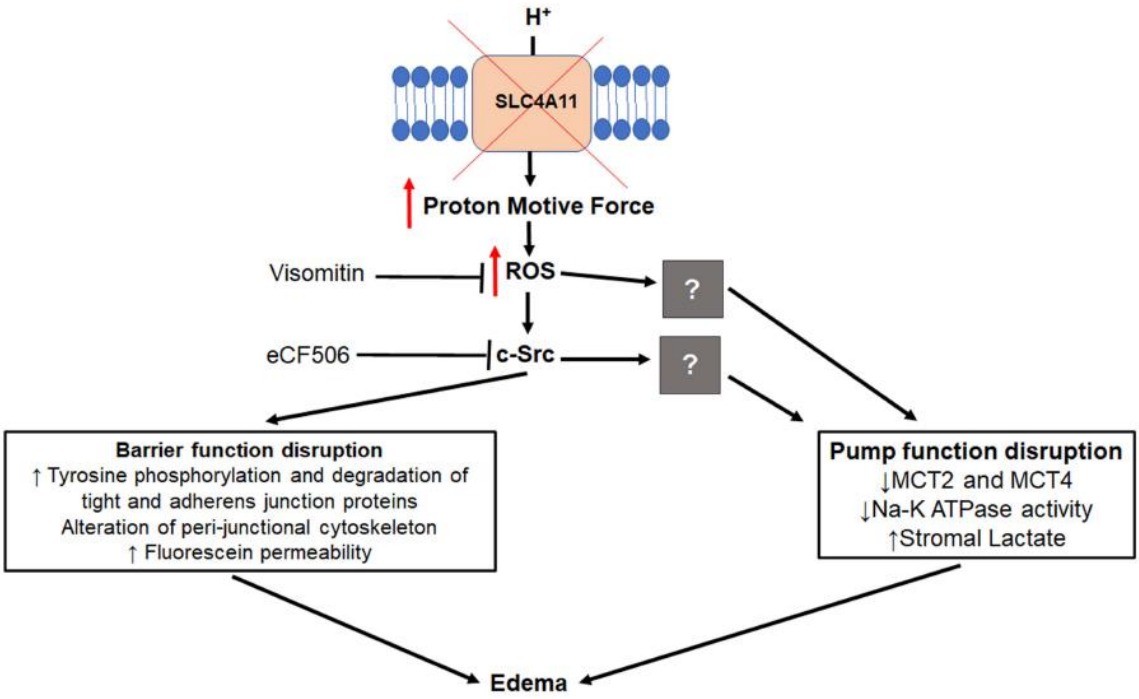

Figure 9. Lack of Slc4a11 leads to increased proton motive force resulting in increased mitoROS. ROS directly activates Src kinase phosphorylating tyrosine residues of tight and adherens junction proteins leading to their degradation and/or mis-localization. Cortical cytoskeleton alterations are induced as a secondary response. The result is perturbation of the barrier function. ROS and Src kinase activation also led to down regulation of MCT2 and MCT4, and decreased Na^+-K^+-ATPase activity with subsequent stromal lactate accumulation resulting in failure of the corneal endothelial pump. The end result is corneal edema.

Funding: Supported by NIH RO1EY031321 and RO1EY008834 to JAB.

Acknowledgements: We thank Catherine K. Cheng for her expert assistance in Jess immunoblot and confocal microscopy techniques and Sangly P. Srinivas for his critique of the manuscript.

Authors Contributions: J.A.B and D.G.O designed the research approach and interpreted experiment results. D.G.O. performed Jess Immunoblots and immunoprecipitations, Na^+/K^+ ATPase assay, immunohistochemistry and MitoSOX staining. E.T.K. and D.G.O. performed OCT imaging. S.L. and E.T.K. performed Lactate measurements. J.A.B. and D.G.O. wrote and edited the manuscript.

Conflicts of Interest: None.

References

1. Vithana, E.N., et al., *Mutations in sodium-borate cotransporter SLC4A11 cause recessive congenital hereditary endothelial dystrophy (CHED2).* Nat Genet, 2006. **38**(7): p. 755-7.
2. Alka, K. and J.R. Casey, *Ophthalmic Nonsteroidal Anti-Inflammatory Drugs as a Therapy for Corneal Dystrophies Caused by SLC4A11 Mutation.* Invest Ophthalmol Vis Sci, 2018. **59**(10): p. 4258-4267.
3. Ogando, D.G., et al., *Ammonia sensitive SLC4A11 mitochondrial uncoupling reduces glutamine induced oxidative stress.* Redox Biol, 2019. **26**: p. 101260.
4. Nehrke, K., *H(OH), H(OH), H(OH): a holiday perspective. Focus on "Mouse Slc4a11 expressed in Xenopus oocytes is an ideally selective H+/OH- conductance pathway that is stimulated by rises in intracellular and extracellular pH".* Am J Physiol Cell Physiol, 2016. **311**(6): p. C942-C944.
5. Shyam, R., et al., *Mitochondrial ROS Induced Lysosomal Dysfunction and Autophagy Impairment in an Animal Model of Congenital Hereditary Endothelial Dystrophy.* Invest Ophthalmol Vis Sci, 2021. **62**(12): p. 15.
6. Han, S.B., et al., *Mice with a targeted disruption of Slc4a11 model the progressive corneal changes of congenital hereditary endothelial dystrophy.* Invest Ophthalmol Vis Sci, 2013. **54**(9): p. 6179-89.

7. Li, S., et al., *Corneal Endothelial Pump Coupling to Lactic Acid Efflux in the Rabbit and Mouse.* Invest Ophthalmol Vis Sci, 2020. **61**(2): p. 7.
8. Ogando, D.G., et al., *Inducible Slc4a11 Knockout Triggers Corneal Edema Through Perturbation of Corneal Endothelial Pump.* Invest Ophthalmol Vis Sci, 2021. **62**(7): p. 28.
9. Bonanno, J.A., *Molecular mechanisms underlying the corneal endothelial pump.* Exp Eye Res, 2012. **95**(1): p. 2-7.
10. Guha, S., et al., *SLC4A11 depletion impairs NRF2 mediated antioxidant signaling and increases reactive oxygen species in human corneal endothelial cells during oxidative stress.* Sci Rep, 2017. **7**(1): p. 4074.
11. Guntaka, S.R., et al., *Epidermal growth factor protects the apical junctional complexes from hydrogen peroxide in bile duct epithelium.* Lab Invest, 2011. **91**(9): p. 1396-409.
12. MacKay, C.E., et al., *ROS-dependent activation of RhoA/Rho-kinase in pulmonary artery: Role of Src-family kinases and ARHGEF1.* Free Radic Biol Med, 2017. **110**: p. 316-331.
13. Zhang, W., et al., *Role of Src in Vascular Hyperpermeability Induced by Advanced Glycation End Products.* Sci Rep, 2015. **5**: p. 14090.
14. Harhaj, N.S., et al., *VEGF activation of protein kinase C stimulates occludin phosphorylation and contributes to endothelial permeability.* Invest Ophthalmol Vis Sci, 2006. **47**(11): p. 5106-15.
15. Shivanna, M., G. Rajashekhar, and S.P. Srinivas, *Barrier dysfunction of the corneal endothelium in response to TNF-alpha: role of p38 MAP kinase.* Invest Ophthalmol Vis Sci, 2010. **51**(3): p. 1575-82.
16. Schweitzer, K.S., et al., *Mechanisms of lung endothelial barrier disruption induced by cigarette smoke: role of oxidative stress and ceramides.* Am J Physiol Lung Cell Mol Physiol, 2011. **301**(6): p. L836-46.
17. Rao, R.K., et al., *Tyrosine phosphorylation and dissociation of occludin-ZO-1 and E-cadherin-beta-catenin complexes from the cytoskeleton by oxidative stress.* Biochem J, 2002. **368**(Pt 2): p. 471-81.
18. Sheth, P., et al., *Lipopolysaccharide disrupts tight junctions in cholangiocyte monolayers by a c-Src-, TLR4-, and LBP-dependent mechanism.* Am J Physiol Gastrointest Liver Physiol, 2007. **293**(1): p. G308-18.
19. Srinivas, S.P., *Dynamic regulation of barrier integrity of the corneal endothelium.* Optom Vis Sci, 2010. **87**(4): p. E239-54.
20. Schlotzer-Schrehardt, U., et al., *Potential Functional Restoration of Corneal Endothelial Cells in Fuchs Endothelial Corneal Dystrophy by ROCK Inhibitor (Ripasudil).* Am J Ophthalmol, 2021. **224**: p. 185-199.
21. Petrov, A., et al., *SkQ1 Ophthalmic Solution for Dry Eye Treatment: Results of a Phase 2 Safety and Efficacy Clinical Study in the Environment and During Challenge in the Controlled Adverse Environment Model.* Adv Ther, 2016. **33**(1): p. 96-115.
22. Wei, Y., et al., *The Role of SKQ1 (Visomitin) in Inflammation and Wound Healing of the Ocular Surface.* Ophthalmol Ther, 2019. **8**(1): p. 63-73.
23. Heppner, D.E., et al., *Direct cysteine sulfenylation drives activation of the Src kinase.* Nat Commun, 2018. **9**(1): p. 4522.
24. Pelaz, S.G. and A. Tabernero, *Src: coordinating metabolism in cancer.* Oncogene, 2022. **41**(45): p. 4917-4928.
25. Chalimeswamy, A., et al., *Oxidative Stress Induces a Breakdown of the Cytoskeleton and Tight Junctions of the Corneal Endothelial Cells.* J Ocul Pharmacol Ther, 2022. **38**(1): p. 74-84.
26. Macsai, M.S. and M. Shiloach, *Use of Topical Rho Kinase Inhibitors in the Treatment of Fuchs Dystrophy After Descemet Stripping Only.* Cornea, 2019. **38**(5): p. 529-534.
27. Fujimoto, H., Y. Setoguchi, and J. Kiryu, *The ROCK Inhibitor Ripasudil Shows an Endothelial Protective Effect in Patients With Low Corneal Endothelial Cell Density After Cataract Surgery.* Transl Vis Sci Technol, 2021. **10**(4): p. 18.
28. Okumura, N., et al., *Rho kinase inhibitor enables cell-based therapy for corneal endothelial dysfunction.* Sci Rep, 2016. **6**: p. 26113.
29. Ogando, D.G. and J.A. Bonanno, *RNA sequencing uncovers alterations in corneal endothelial metabolism, pump and barrier functions of Slc4a11 KO mice.* Exp Eye Res, 2022. **214**: p. 108884.